

USM-TH-81 //hep-ph/9907556

# Flavor and Spin Structure of Octet Baryons at Large $x$

Bo-Qiang Ma<sup>a</sup>, Ivan Schmidt<sup>b</sup>, and Jian-Jun Yang<sup>b,c</sup>

<sup>a</sup>Department of Physics, Peking University, Beijing 100871, China,\*  
 CCAST (World Laboratory), P.O. Box 8730, Beijing 100080, China,  
 and Institute of High Energy Physics, Academia Sinica, P. O. Box 918(4),  
 Beijing 100039, China

e-mail: mabq@phy.pku.edu.cn

<sup>b</sup>Departamento de Física, Universidad Técnica Federico Santa María,  
 Casilla 110-V, Valparaíso, Chile  
 Email: ischmidt@fis.utfsm.cl

<sup>c</sup>Department of Physics, Nanjing Normal University,  
 Nanjing 210097, China  
 Email: jjyang@fis.utfsm.cl

## Abstract

The quark flavor and spin distributions in octet baryons are calculated both in the SU(6) quark spectator diquark model and in a perturbative QCD (pQCD) based model. It is shown that the  $\Lambda$  has the most significant difference in flavor structure at large  $x$  between the two models, though the flavor and spin structure of other baryons can also provide tests of different models. The Drell-Yan process for  $\Sigma^\pm$  beams on isoscalar targets can be used to test different predictions concerning the valence quark flavor structure of the  $\Sigma^\pm$ .

PACS numbers: 14.20.-c, 12.38.Bx, 12.39.Ki, 13.85.-t

Published in Nucl. Phys. B 574 (2000) 331

---

\*Mailing address

# 1 Introduction

Parton distributions of hadrons and the formation of hadrons from fragmentation of partons are of considerable current interest in the community of particle and nuclear physics. There have been remarkable achievements in our knowledge of the quark-gluon structure of the nucleon from three decades of experimental and theoretical investigations in various deep inelastic scattering (DIS) processes. However, there are still a number of unknowns concerning the detailed flavor and spin structure of the nucleon, such as the detailed origin of the proton spin [1], the strange content of the nucleon [2, 3], the flavor asymmetry of the sea [4], the isospin symmetry breaking at small  $x$  [5], and the flavor and spin structure of the valence quarks at large  $x$  [6, 7, 8, 9, 10, 11]. It is important to perform high precision measurements of available physical quantities and/or to measure new quantities related to the flavor and spin structure of the nucleons, in order to have a better understanding of the quark-gluon structure of the nucleon. Nevertheless, it has recently been found [12] that the flavor and spin structure of the  $\Lambda$ -hyperon may serve as a new domain where the same physics that governs the structure of the nucleon can manifest itself. It was found that the flavor and spin structure of the quark distributions of the  $\Lambda$  differ significantly at large  $x$  from a perturbative QCD (pQCD) based analysis and a SU(6) quark-diquark model. A detailed analysis [13] of the available  $\Lambda$ -polarization data in  $e^+e^-$  annihilation at the  $Z$ -pole supports the prediction that the  $u$  and  $d$  quarks inside the  $\Lambda$  should be positively polarized at large  $x$ , though their net helicities might be zero or negative. The most recent HERMES result [14] of spin transfer to the  $\Lambda$  in deep elastic scattering of polarized lepton on the nucleon target also support the predictions of the SU(6) quark-diquark model and the pQCD based model [12].

The direct measurements of the  $\Lambda$  quark structure are not easy since it is a charged neutral particle which cannot be accelerated as incident beam and its short life time makes it also difficult to be used as target. The simple reciprocity relation [15]

$$q_h(x) \propto D_q^h(z), \quad (1)$$

where  $z = 2p \cdot q/Q^2$  is the momentum fraction of the produced hadron from the

quark jet in the fragmentation process and  $x = Q^2/2p \cdot q$  is the Bjorken scaling variable corresponding to the momentum fraction of the quark from the hadron in the DIS process, can provide a reasonable connection between different physical quantities and lead to understandings of the  $\Lambda$  quark structure from the various quark to  $\Lambda$  fragmentations. However, such a relation is still not completely free from theoretical and experimentally uncertainties, though it may serve for our purpose as an approximate qualitative connection at a specific scale  $Q^2$ , near  $x \rightarrow 1$  and  $z \rightarrow 1$  [16, 17]. Thus the direct measurement of the quark structure of other octet baryons other than the nucleon and  $\Lambda$  has a strong physical significance, and can provide a new direction to test different theories concerning the nucleon structure.

The purpose of this paper is to extend the analysis of the quark structure from the nucleon and  $\Lambda$  cases to the other members of octet baryons. We will calculate the quark distributions for all of the octet baryons in the SU(6) quark spectator diquark model and in a perturbative QCD based model. There are two motivations for such a study: (1) to check the difference in flavor and spin structure of all octet baryons between the two models, and see which baryon has the most significant difference; (2) some charged baryons other than nucleons, such as  $\Sigma^\pm$ , may be used as beam to directly measure their own quark structure in case the structure of the target is comparatively well known. We will find that the  $\Lambda$  has the most significant difference at large  $x$  in the flavor and spin structure for a clean test of different predictions. We will also show that the  $\Sigma$ 's have the most significant difference in the flavor and spin structure between the two models at medium to large  $x$ , and the measurement of Drell-Yan process for  $\Sigma^\pm$  beams on the isoscalar targets can test different predictions of the quark structure of the  $\Sigma^\pm$  baryons. It is more appealing that the  $\Lambda$  and  $\Sigma^0$  have complete different flavor and spin structure though they are composed of same flavor quarks.

We shall start Sec. II with the presentation of quark distributions of octet baryons in the SU(6) quark-diquark spectator model and in a perturbative QCD based model. We then compare the flavor and spin structure of all the octet baryons between the two models at large  $x$ . Then in Sec. III, we present the formulas for the Drell-Yan process using  $\Sigma^\pm$  beams on isoscalar targets and show different predictions of cross

section ratios in the pQCD based model and in the quark spectator diquark model. Finally, we present conclusions in Section IV.

## 2 The Quark Spin and Flavor Structure of Octet Baryons

In this section, we extend the analysis of the quark structure of nucleons to all members of octet baryons using (1) the SU(6) quark spectator diquark model and, (2) a perturbative QCD (pQCD) based model.

### 2.1 SU(6) Quark Spectator Diquark Model

Before we look into the details of the spin and the flavor structure for the valence quarks of the octet baryons, we briefly review the analysis of the unpolarized and polarized quark distributions of nucleons in the light-cone SU(6) quark-spectator-diquark model [9]. As we know, it is proper to describe deep inelastic scattering as the sum of incoherent scatterings of the incident lepton on the partons in the infinite momentum frame or in the light-cone formalism. The unpolarized valence quark distributions  $u_v(x)$  and  $d_v(x)$  of the proton are given in this model by

$$\begin{aligned} u_v(x) &= \frac{1}{2}a_S(x) + \frac{1}{6}a_V(x); \\ d_v(x) &= \frac{1}{3}a_V(x), \end{aligned} \quad (2)$$

where  $a_D(x)$  ( $D = S$  for scalar spectator or  $V$  for axial vector spectator) can be expressed in terms of the light-cone momentum space wave function  $\varphi(x, \vec{k}_\perp)$  as

$$a_D(x) \propto \int [d^2 \vec{k}_\perp] |\varphi(x, \vec{k}_\perp)|^2, \quad (D = S \text{ or } V) \quad (3)$$

which is normalized such that  $\int_0^1 dx a_D(x) = 3$  and denotes the amplitude for quark  $q$  to be scattered while the spectator is in the diquark state  $D$ .

The quark helicity distributions for the  $u$  and  $d$  quarks in the proton can be

written as [9]

$$\begin{aligned}\Delta u_v(x) &= u_v^\uparrow(x) - u_v^\downarrow(x) = -\frac{1}{18}a_V(x)W_V(x) + \frac{1}{2}a_S(x)W_S(x); \\ \Delta d_v(x) &= d_v^\uparrow(x) - d_v^\downarrow(x) = -\frac{1}{9}a_V(x)W_V(x),\end{aligned}\quad (4)$$

in which  $W_V(x)$  and  $W_S(x)$  are the Melosh-Wigner correction factors [18] for the axial vector and scalar spectator-diquark cases. They are obtained by averaging

$$W_D(x, \mathbf{k}_\perp) = \frac{(k^+ + m_q)^2 - \mathbf{k}_\perp^2}{(k^+ + m_q)^2 + \mathbf{k}_\perp^2}, \quad (5)$$

over  $\mathbf{k}_\perp$  with  $k^+ = x\mathcal{M}$  and  $\mathcal{M}^2 = \frac{m_q^2 + \mathbf{k}_\perp^2}{x} + \frac{m_D^2 + \mathbf{k}_\perp^2}{1-x}$ , where  $m_D$  is the mass of the diquark spectator, and are unequal due to unequal spectator masses, which leads to unequal  $\mathbf{k}_\perp$  distributions.

Now, we extend the above analysis of the valence quark distributions of the proton to that of the octet baryons. The valence quark distributions of the  $\Lambda$  in the SU(6) quark spectator diquark model have been analyzed in detail in Ref.[13]. The  $\Lambda$  wave function in the conventional SU(6) quark model is written as

$$|\Lambda^\uparrow\rangle = \frac{1}{2\sqrt{3}}[(u^\uparrow d^\downarrow + d^\downarrow u^\uparrow) - (u^\downarrow d^\uparrow + d^\uparrow u^\downarrow)]s^\uparrow + (\text{cyclic permutation}). \quad (6)$$

The SU(6) quark-diquark model wave function for the  $\Lambda$  is written as

$$\Psi_\Lambda^{\uparrow,\downarrow} = \sin\theta \varphi_V |qV\rangle_\Lambda^{\uparrow,\downarrow} + \cos\theta \varphi_S |qS\rangle_\Lambda^{\uparrow,\downarrow}, \quad (7)$$

with

$$\begin{aligned}|qV\rangle_\Lambda^{\uparrow,\downarrow} &= \pm\frac{1}{\sqrt{6}}[V_0(ds)u^{\uparrow,\downarrow} - V_0(us)d^{\uparrow,\downarrow} - \sqrt{2}V_\pm(ds)u^{\downarrow,\uparrow} + \sqrt{2}V_\pm(us)d^{\downarrow,\uparrow}]; \\ |qS\rangle_\Lambda^{\uparrow,\downarrow} &= \frac{1}{\sqrt{6}}[S(ds)u^{\uparrow,\downarrow} + S(us)d^{\uparrow,\downarrow} - 2S(us)d^{\downarrow,\uparrow}],\end{aligned}\quad (8)$$

where  $V_{s_z}(q_1 q_2)$  stands for a  $q_1 q_2$  vector diquark Fock state with third spin component  $s_z$ ,  $S(q_1 q_2)$  stands for a  $q_1 q_2$  scalar diquark Fock state, and  $\varphi_D$  stands for the momentum space wave function of the quark-diquark with  $D$  representing the vector (V) or scalar (S) diquarks. The angle  $\theta$  is a mixing angle that breaks the SU(6) symmetry at  $\theta \neq \pi/4$  and in this paper we choose the bulk SU(6) symmetry case  $\theta = \pi/4$ .

We analyze the valence quark distributions of the  $\Sigma^0$  by extending the SU(6) quark-spectator-diquark model from the nucleon [9] and  $\Lambda$  [13] cases to the  $\Sigma^0$ . Similarly, the  $\Sigma^0$  wave function in the conventional SU(6) quark model is

$$\begin{aligned}
|\Sigma^{0\uparrow}\rangle &= \frac{1}{3}(u^\uparrow d^\uparrow + d^\uparrow u^\uparrow)s^\downarrow \\
&- \frac{1}{6}(u^\uparrow d^\downarrow + u^\downarrow d^\uparrow + d^\uparrow u^\downarrow + d^\downarrow u^\uparrow)s^\uparrow + (\text{cyclic permutation}). \quad (9)
\end{aligned}$$

The SU(6) quark-diquark model wave function for the  $\Sigma^0$  is written as

$$\Psi_{\Sigma^0}^{\uparrow\downarrow} = \sin \theta \varphi_V |qV\rangle_{\Sigma^0}^{\uparrow\downarrow} + \cos \theta \varphi_S |qS\rangle_{\Sigma^0}^{\uparrow\downarrow}, \quad (10)$$

with

$$\begin{aligned}
|qV\rangle_{\Sigma^0}^{\uparrow\downarrow} &= \pm \frac{1}{3}[\sqrt{2}V_0(ud)s^{\uparrow,\downarrow} - \frac{1}{\sqrt{2}}V_0(us)d^{\uparrow,\downarrow} - \frac{1}{\sqrt{2}}V_0(ds)u^{\uparrow,\downarrow} \\
&- 2V_\pm(ud)s^{\downarrow,\uparrow} + V_\pm(us)d^{\downarrow,\uparrow} + V_\pm(ds)u^{\downarrow,\uparrow}]; \quad (11)
\end{aligned}$$

$$|qS\rangle_{\Sigma^0}^{\uparrow\downarrow} = -\frac{1}{\sqrt{2}}[S(us)d^{\uparrow,\downarrow} + S(ds)u^{\uparrow,\downarrow}]. \quad (12)$$

Instead of writing the wave functions for other octet baryons as above, in Tab. 1 we present all quark distributions of octet baryons in SU(6) quark spectator diquark model with the quark-diquark amplitude  $a_D$  with  $D = V, S$ . The Melosh-Wigner rotation effect in the quark spin distributions is denoted by the amplitude

$$\tilde{a}_D = a_D(x)W_D(x), \quad (13)$$

In the calculation, we employ the Brodsky-Huang-Lepage (BHL) prescription [19] of the light-cone momentum space wave function for the quark-spectator

$$\varphi(x, \vec{k}_\perp) = A_D \exp\left\{-\frac{1}{8\alpha_D^2}\left[\frac{m_q^2 + \vec{k}_\perp^2}{x} + \frac{m_D^2 + \vec{k}_\perp^2}{1-x}\right]\right\}, \quad (14)$$

with the parameter  $\alpha_D = 330$ . Other parameters such as the quark mass  $m_q$ , vector(scalar) diquark mass  $m_{V(S)}$  for baryons of the octet are listed in the table.

The quark structure of the other members of the octet baryons are connected to the proton by SU(3) symmetry with the valence quarks  $q_1 = u$  and  $q_2 = d$  for proton replaced by  $q_1$  and  $q_2$  in Tab. 2 for the corresponding baryon. In the quark spectator diquark model the exact SU(3) symmetry is broken due to the mass difference for different quarks and diquarks, as shown in Tab.1.

Table 1 The quark distribution functions of octet baryons in SU(6) quark-diquark model

Baryon	$q$		$\Delta q$		$m_q$ (MeV)	$m_V$ (MeV)	$m_S$ (MeV)
p (uud)	$u$	$\frac{1}{6}a_V + \frac{1}{2}a_S$	$\Delta u$	$-\frac{1}{18}\tilde{a}_V + \frac{1}{2}\tilde{a}_S$	330	800	600
	$d$	$\frac{1}{3}a_V$	$\Delta d$	$-\frac{1}{9}\tilde{a}_V$	330	800	600
n (udd)	$u$	$\frac{1}{3}a_V$	$\Delta u$	$-\frac{1}{9}\tilde{a}_V$	330	800	600
	$d$	$\frac{1}{6}a_V + \frac{1}{2}a_S$	$\Delta d$	$-\frac{1}{18}\tilde{a}_V + \frac{1}{2}\tilde{a}_S$	330	800	600
$\Sigma^+$ (uus)	$u$	$\frac{1}{6}a_V + \frac{1}{2}a_S$	$\Delta u$	$-\frac{1}{18}\tilde{a}_V + \frac{1}{2}\tilde{a}_S$	330	950	750
	$s$	$\frac{1}{3}a_V$	$\Delta s$	$-\frac{1}{9}\tilde{a}_V$	480	800	600
$\Sigma^0$ (uds)	$u$	$\frac{1}{12}a_V + \frac{1}{4}a_S$	$\Delta u$	$-\frac{1}{36}\tilde{a}_V + \frac{1}{4}\tilde{a}_S$	330	950	750
	$d$	$\frac{1}{12}a_V + \frac{1}{4}a_S$	$\Delta d$	$-\frac{1}{36}\tilde{a}_V + \frac{1}{4}\tilde{a}_S$	330	950	750
	$s$	$\frac{1}{3}a_V$	$\Delta s$	$-\frac{1}{9}\tilde{a}_V$	480	800	600
$\Sigma^-$ (dds)	$d$	$\frac{1}{6}a_V + \frac{1}{2}a_S$	$\Delta d$	$-\frac{1}{18}\tilde{a}_V + \frac{1}{2}\tilde{a}_S$	330	950	750
	$s$	$\frac{1}{3}a_V$	$\Delta s$	$-\frac{1}{9}\tilde{a}_V$	480	800	600
$\Lambda^0$ (uds)	$u$	$\frac{1}{4}a_V + \frac{1}{12}a_S$	$\Delta u$	$-\frac{1}{12}\tilde{a}_V + \frac{1}{12}\tilde{a}_S$	330	950	750
	$d$	$\frac{1}{4}a_V + \frac{1}{12}a_S$	$\Delta d$	$-\frac{1}{12}\tilde{a}_V + \frac{1}{12}\tilde{a}_S$	330	950	750
	$s$	$\frac{1}{3}a_S$	$\Delta s$	$\frac{1}{3}\tilde{a}_S$	480	800	600
$\Xi^-$ (dss)	$d$	$\frac{1}{3}a_V$	$\Delta d$	$-\frac{1}{9}\tilde{a}_V$	330	1100	900
	$s$	$\frac{1}{6}a_V + \frac{1}{2}a_S$	$\Delta s$	$-\frac{1}{18}\tilde{a}_V + \frac{1}{2}\tilde{a}_S$	480	950	750
$\Xi^0$ (uss)	$u$	$\frac{1}{3}a_V$	$\Delta u$	$-\frac{1}{9}\tilde{a}_V$	330	1100	900
	$s$	$\frac{1}{6}a_V + \frac{1}{2}a_S$	$\Delta s$	$-\frac{1}{18}\tilde{a}_V + \frac{1}{2}\tilde{a}_S$	480	950	750

The quark distributions in baryons of the octet which can be calculated by using the parameters in Tab. 1, are shown in Figs. 1-8 (  $q_1$  and  $q_2$  for all octet baryons are specified in Tab. 2 ). We need to mention that our results are consistent with a recent calculation of the quark structure of the octet baryons in the MIT bag model [20], though there are some differences in the detailed features.

## 2.2 Perturbative QCD Method

We now extend the pQCD analysis of the quark structure of baryons from the  $\Lambda$  case [13] to all of the octet baryons. We adopt the canonical form for the quark

distributions, following Ref. [8],

$$\begin{aligned} q_i^\uparrow(x) &= \frac{\tilde{A}_{q_i}}{B_3} x^{-\frac{1}{2}} (1-x)^3 + \frac{\tilde{B}_{q_i}}{B_4} x^{-\frac{1}{2}} (1-x)^4; \\ q_i^\downarrow(x) &= \frac{\tilde{C}_{q_i}}{B_5} x^{-\frac{1}{2}} (1-x)^5 + \frac{\tilde{D}_{q_i}}{B_6} x^{-\frac{1}{2}} (1-x)^6. \end{aligned} \quad (15)$$

with  $i = 1, 2$ , where  $B_n = B(1/2, n+1)$  is the  $\beta$ -function defined by  $B(1-\alpha, n+1) = \int_0^1 x^{-\alpha} (1-x)^n dx$  for  $\alpha = 1/2$ . From (15), we obtain the valence quark normalization for quark  $q_i$

$$N_i = \tilde{A}_{q_i} + \tilde{B}_{q_i} + \tilde{C}_{q_i} + \tilde{D}_{q_i}, \quad (16)$$

and the corresponding polarized distribution in the  $J^p = \frac{1}{2}^+$  octet

$$\Delta Q_i = \tilde{A}_{q_i} + \tilde{B}_{q_i} - \tilde{C}_{q_i} - \tilde{D}_{q_i}, \quad (17)$$

which can be extracted by using SU(3) symmetry from  $\Sigma Q_i = \Delta u + \Delta d + \Delta s \approx 0.20$  obtained in deep-inelastic lepton-proton scattering experiments [21] and the constants  $F = 0.459$  and  $D = 0.798$  obtained from hyperon decay experiments [22].

In a strict sense, the  $\Delta Q_i$  obtained this way from SU(3) symmetry of the octet baryons should include both the contributions from the valence and sea quarks. However, we know from the recent measurements from semi-inclusive charged meson production in DIS process [23, 24] that the sea polarizations are consistent with zero, and the measured  $\Delta u$  and  $\Delta d$  for the valence quarks are close to the  $\Delta u$  and  $\Delta d$  above. We may simply adopt the pQCD case 2 of Ref.[13] with only the leading term for valence quarks (i.e., we set  $B_i = 0$  and  $D_i = 0$ ) as an example for the pQCD predictions of the quark distributions. However, to reflect the situation that the real quark distributions are actually more complicated, we shall adopt the pQCD case 3 with the quark helicity sums  $\Delta Q_1$  and  $\Delta Q_2$  as given in Tab. 2 to parameterize the quark distributions, based on the above forms Eq. (15) for the valence quark distributions.

In Tab. 2, the ratio

$$R_A = \frac{\tilde{A}_{q_2}}{\tilde{A}_{q_1}} \quad (18)$$

reflects the  $x \rightarrow 1$  behaviour of  $\frac{q_2^\uparrow}{q_1^\uparrow}(x)$  in a baryon. For every baryon, there are five constraints given by Eqs.(16)-(18), which then result in three free parameters, chosen as  $\tilde{A}_{q_1}$ ,  $\tilde{C}_{q_1}$  and  $\tilde{C}_{q_2}$ , which should be actually further constrained by relevant

data. Here we are not intend to determine these parameters with their exact values. However, we find, as an example, one set of parameters with the values  $\tilde{A}_{q_1} = 5$ ,  $\tilde{C}_{q_1} = 3$  and  $\tilde{C}_{q_2} = 2$  for the nucleon can give a rough shape of quark flavor and spin distributions in the nucleon. We also find that the parameters with the values  $\tilde{A}_{q_1} = 2$ ,  $\tilde{C}_{q_1} = 2$  and  $\tilde{C}_{q_2} = 2$  for the  $\Lambda$  can be used to give a good description of the  $\Lambda$ -polarization [13]. Since we know little about the quark distributions in the  $\Sigma^0$ , its input parameters are taken to be the same as those for the  $\Lambda^0$ . The input parameters for the other octet baryons are taken to be the same as the nucleon in consideration of the symmetry among them. All other parameters determined according to the constraint conditions are listed in Tab. 2.

Table 2 The parameters for quark distributions of octet baryons in pQCD

Baryon	$q_1$	$q_2$	$R_A$	$\Delta Q_1$	$\Delta Q_2$	$\tilde{A}_{q_1}$	$\tilde{B}_{q_1}$	$\tilde{C}_{q_1}$	$\tilde{D}_{q_1}$	$\tilde{A}_{q_2}$	$\tilde{B}_{q_2}$	$\tilde{C}_{q_2}$	$\tilde{D}_{q_2}$
p	u	d	$\frac{1}{5}$	0.79	-0.47	5.0	-3.61	3.0	-2.40	1.0	-0.74	2.0	-1.27
n	d	u	$\frac{1}{5}$	0.79	-0.47	5.0	-3.61	3.0	-2.40	1.0	-0.74	2.0	-1.27
$\Sigma^+$	u	s	$\frac{1}{5}$	0.79	-0.47	5.0	-3.61	3.0	-2.40	1.0	-0.74	2.0	-1.27
$\Sigma^0$	u(d)	s	$\frac{2}{5}$	0.33	-0.47	2.0	-1.34	2.0	-1.67	0.8	-0.54	2.0	-1.27
$\Sigma^-$	d	s	$\frac{1}{5}$	0.79	-0.47	5.0	-3.61	3.0	-2.40	1.0	-0.74	2.0	-1.27
$\Lambda^0$	s	u(d)	$\frac{1}{2}$	0.60	-0.20	2.0	-1.20	2.0	-1.80	1.0	-0.60	2.0	-1.40
$\Xi^-$	s	d	$\frac{1}{5}$	0.79	-0.47	5.0	-3.61	3.0	-2.40	1.0	-0.74	2.0	-1.27
$\Xi^0$	s	u	$\frac{1}{5}$	0.79	-0.47	5.0	-3.61	3.0	-2.40	1.0	-0.74	2.0	-1.27

The quark distributions in octet baryons calculated according to the parameters in Tab. 2 are shown in Figs. 1-8. By comparing the results (see Figs.1-8) obtained by using the SU(6) quark-diquark model and the pQCD based model, one can find the following interesting features at  $x \rightarrow 1$ , for all of the other octet baryons besides  $\Lambda^0$ :

$$\begin{cases} \left(\frac{\Delta q_2(x)}{q_2(x)}\right)_{Diquark} \rightarrow -\frac{1}{3}; \\ \left(\frac{\Delta q_2(x)}{q_2(x)}\right)_{pQCD} \rightarrow 1. \end{cases}$$

In addition, the two models also predict different quark flavor structures

$$\begin{cases} \left(\frac{q_2(x)}{q_1(x)}\right)_{Diquark} \rightarrow 0; \\ \left(\frac{q_2(x)}{q_1(x)}\right)_{pQCD} \rightarrow \frac{1}{5}, \end{cases}$$

for all other octet baryons besides  $\Sigma^0$  and  $\Lambda$ . This corresponds to  $s(x)/u(x)$  in  $\Sigma^\pm$ .

In case of the  $\Sigma^0$  with  $q_1 = u, d$  and  $q_2 = s$ , we find

$$\begin{cases} \left(\frac{q_2(x)}{q_1(x)}\right)_{Diquark} \rightarrow 0; \\ \left(\frac{q_2(x)}{q_1(x)}\right)_{pQCD} \rightarrow \frac{2}{5}, \end{cases}$$

which is with bigger difference of the flavor structure at large  $x$  between the two models. However, for the  $\Lambda$  with  $q_1 = s$  and  $q_2 = u, d$ , we know that [12, 13]

$$\begin{cases} \left(\frac{q_2(x)}{q_1(x)}\right)_{Diquark} \rightarrow 0; \\ \left(\frac{q_2(x)}{q_1(x)}\right)_{pQCD} \rightarrow \frac{1}{2}, \end{cases}$$

which has the largest difference in the flavor structure at large  $x$  between the two models among all the baryons. This supports the conclusion in Ref.[12] that the spin and flavor structure for the  $\Lambda$  can provide a clean test of different models. We notice that  $q_1$  in Tab. 2 in both models is the dominant quark contributing to the main spin and valence structure at large  $x$ , and also that:

$$\begin{cases} \left(\frac{\Delta q_1(x)}{q_1(x)}\right)_{Diquark} \rightarrow 1; \\ \left(\frac{\Delta q_1(x)}{q_1(x)}\right)_{pQCD} \rightarrow 1. \end{cases}$$

Therefore the difference between the two models mainly come from the valence quark  $q_2$ . We have also neglected the contribution of sea quarks and their polarizations, although they may have small contribution at small  $x$ .

It is interesting to notice that the  $\Sigma$ 's have the most significant difference in the flavor and spin structure between the two models at medium to large  $x$  region and this feature makes it possible to have tests between pQCD and the quark-diquark model predictions, as we will discuss in the following section. It is even more appealing that the  $\Lambda$  and  $\Sigma^0$  have complete different flavor and spin structure (remember also that  $q_1 = u, d$  and  $q_2 = s$  for the  $\Sigma^0$  whereas  $q_1 = s$  and  $q_2 = u, d$  for the  $\Lambda$ ) though they are composed of same flavor quarks. Thus it is more novel to check the different predictions concerning the flavor and spin structure of the  $\Lambda$  and  $\Sigma^0$ , or  $\Sigma^\pm$ . The  $\Sigma^\pm$  has close flavor structure compared to that of  $\Sigma^0$  (even we chose different sets of input parameters as can be found from Tab. 2), thus measurement of  $\Sigma^\pm$  is also helpful for our understanding of the  $\Sigma^0$  structure.

### 3 Drell-Yan Process for $\Sigma^\pm$ Beams on Isoscalar Targets

Although the  $\Lambda$  can provide a clean test of the different flavor and spin structure between the two different models, it is still not possible to make a clear distinction between the above two predictions with the available data of the  $\Lambda$ -polarization in the  $e^+e^-$  process near the  $Z$ -pole [13]. We also need a connection between the quark distributions inside the  $\Lambda$  and the quark fragmentation into a  $\Lambda$  and such a connection is still not free from theoretical and experimental uncertainties. As we pointed out in the introduction, direct measurement of the quark structure of a charged octet baryon is free from the requirement of a connection between the quark distributions and the quark fragmentation functions, in order to study the quark structure of other baryons other than the nucleon. It was also pointed out in Ref.[12] that the charged particles,  $\Sigma^\pm$  or  $\Xi^-$ , may be used as beam in the Drell-Yan process, to test different predictions concerning the quark structure of the involved baryons. The Drell-Yan process has been widely used experimentally to study the quark structure of the nucleon [25]. Using the  $\Sigma^\pm$  as beam in Drell-Yan processes has been suggested [26] for the purpose of studying the flavor asymmetry in the sea of the baryons. In this section, we consider the Drell-Yan process for  $\Sigma^\pm$  on isoscalar targets and show that it is also a useful tool in order to study the flavor structure of  $\Sigma^\pm$  at medium to large  $x$ , in order to test different predictions of the pQCD model and the quark spectator diquark model.

For the process

$$\Sigma N \rightarrow l^+ l^- X, \quad (19)$$

the cross section can be written as

$$\sigma(\Sigma N) = \frac{8\pi\alpha^2}{9\sqrt{\tau}} K(x_1, x_2) \sum_f e_f^2 [q_f^\Sigma(x_1) \bar{q}_f(x_2) + \bar{q}_f^\Sigma(x_1) q_f(x_2)], \quad (20)$$

where  $\sqrt{\tau} = M/\sqrt{s}$ ,  $M$  is the mass of the dilepton pair. The factor  $K(x_1, x_2)$  is due to higher-order QCD corrections. More specifically,

$$\sigma(\Sigma^+ p) = \frac{8\pi\alpha^2}{9\sqrt{\tau}} K(x_1, x_2) \left\{ \frac{4}{9} [u^{\Sigma^+}(x_1) \bar{u}(x_2) + \bar{u}^{\Sigma^+}(x_1) u(x_2)] \right.$$

$$\begin{aligned}
&+ \frac{1}{9} [d^{\Sigma^+}(x_1) \bar{d}(x_2) + \bar{d}^{\Sigma^+}(x_1) d(x_2)] \\
&+ \frac{1}{9} [s^{\Sigma^+}(x_1) \bar{s}(x_2) + \bar{s}^{\Sigma^+}(x_1) s(x_2)], \tag{21}
\end{aligned}$$

and

$$\begin{aligned}
\sigma(\Sigma^+ n) &= \frac{8\pi\alpha^2}{9\sqrt{\tau}} K(x_1, x_2) \left\{ \frac{4}{9} [u^{\Sigma^+}(x_1) \bar{d}(x_2) + \bar{u}^{\Sigma^+}(x_1) d(x_2)] \right. \\
&+ \frac{1}{9} [d^{\Sigma^+}(x_1) \bar{u}(x_2) + \bar{d}^{\Sigma^+}(x_1) u(x_2)] \\
&\left. + \frac{1}{9} [s^{\Sigma^+}(x_1) \bar{s}(x_2) + \bar{s}^{\Sigma^+}(x_1) s(x_2)] \right\}. \tag{22}
\end{aligned}$$

By using charge symmetry, i.e.,  $u^{\Sigma^+} \leftrightarrow d^{\Sigma^-}$ ,  $d^{\Sigma^+} \leftrightarrow u^{\Sigma^-}$ ,  $\bar{u}^{\Sigma^+} \leftrightarrow \bar{d}^{\Sigma^-}$ , and  $\bar{d}^{\Sigma^+} \leftrightarrow \bar{u}^{\Sigma^-}$ , one can obtain the cross section of  $\Sigma^- N$  as

$$\begin{aligned}
\sigma(\Sigma^- p) &= \frac{8\pi\alpha^2}{9\sqrt{\tau}} K(x_1, x_2) \left\{ \frac{1}{9} [u^{\Sigma^+}(x_1) \bar{d}(x_2) + \bar{u}^{\Sigma^+}(x_1) d(x_2)] \right. \\
&+ \frac{4}{9} [d^{\Sigma^+}(x_1) \bar{u}(x_2) + \bar{d}^{\Sigma^+}(x_1) u(x_2)] \\
&\left. + \frac{1}{9} [s^{\Sigma^+}(x_1) \bar{s}(x_2) + \bar{s}^{\Sigma^+}(x_1) s(x_2)] \right\}, \tag{23}
\end{aligned}$$

and

$$\begin{aligned}
\sigma(\Sigma^- n) &= \frac{8\pi\alpha^2}{9\sqrt{\tau}} K(x_1, x_2) \left\{ \frac{1}{9} [u^{\Sigma^+}(x_1) \bar{u}(x_2) + \bar{u}^{\Sigma^+}(x_1) u(x_2)] \right. \\
&+ \frac{4}{9} [d^{\Sigma^+}(x_1) \bar{d}(x_2) + \bar{d}^{\Sigma^+}(x_1) d(x_2)] \\
&\left. + \frac{1}{9} [s^{\Sigma^+}(x_1) \bar{s}(x_2) + \bar{s}^{\Sigma^+}(x_1) s(x_2)] \right\}. \tag{24}
\end{aligned}$$

Considering an isoscalar target with the nucleon number of  $A$ , we obtain the cross section

$$\begin{aligned}
\sigma^+ = \sigma(\Sigma^+ A) &= \frac{8\pi\alpha^2}{9\sqrt{\tau}} \frac{A}{2} K(x_1, x_2) \left\{ \frac{4}{9} [u^{\Sigma^+}(x_1) \bar{u}(x_2) + \bar{u}^{\Sigma^+}(x_1) u(x_2)] \right. \\
&+ u^{\Sigma^+}(x_1) \bar{d}(x_2) + \bar{u}^{\Sigma^+}(x_1) d(x_2)] \\
&+ \frac{1}{9} [d^{\Sigma^+}(x_1) \bar{d}(x_2) + d^{\Sigma^+}(x_1) \bar{u}(x_2) + \bar{d}^{\Sigma^+}(x_1) d(x_2) + \bar{d}^{\Sigma^+}(x_1) u(x_2)] \\
&\left. + \frac{1}{9} [2s^{\Sigma^+}(x_1) \bar{s}(x_2) + 2\bar{s}^{\Sigma^+}(x_1) s(x_2)] \right\}; \tag{25}
\end{aligned}$$

$$\begin{aligned}
\sigma^- = \sigma(\Sigma^- A) &= \frac{8\pi\alpha^2 A}{9\sqrt{\tau}} \frac{1}{2} K(x_1, x_2) \{ \frac{1}{9} [u^{\Sigma^+}(x_1) \bar{d}(x_2) + \bar{u}^{\Sigma^+}(x_1) d(x_2) \\
&+ u^{\Sigma^+}(x_1) \bar{u}(x_2) + \bar{u}^{\Sigma^+}(x_1) u(x_2)] \\
&+ \frac{4}{9} [d^{\Sigma^+}(x_1) \bar{u}(x_2) + d^{\Sigma^+}(x_1) \bar{d}(x_2) + \bar{d}^{\Sigma^+}(x_1) u(x_2) + \bar{d}^{\Sigma^+}(x_1) d(x_2)] \\
&+ \frac{4}{9} [2s^{\Sigma^+}(x_1) \bar{s}(x_2) + 2\bar{s}^{\Sigma^+}(x_1) s(x_2)] \}. \tag{26}
\end{aligned}$$

Choice of different ranges of the variables  $x_1$  and  $x_2$  and different combination of the targets with different isospin properties can help us to pin down the information for the various quark distributions of the  $\Sigma^\pm$ . The purpose of this paper is to study the valence quark structure of the  $\Sigma^\pm$  at medium to large  $x$ . Considering the fact that valence quarks dominate in the hyperons at medium to large  $x$ , we obtain

$$\tilde{\sigma}^+(x_1, x_2) = \frac{8\pi\alpha^2 A}{9\sqrt{\tau}} \frac{1}{2} K(x_1, x_2) \{ \frac{4}{9} [u^{\Sigma^+}(x_1) [\bar{u}(x_2) + \bar{d}(x_2)] + \frac{2}{9} s^{\Sigma^+}(x_1) \bar{s}(x_2) \}; \tag{27}$$

$$\tilde{\sigma}^-(x_1, x_2) = \frac{8\pi\alpha^2 A}{9\sqrt{\tau}} \frac{1}{2} K(x_1, x_2) \{ \frac{1}{9} u^{\Sigma^+}(x_1) [\bar{u}(x_2) + \bar{d}(x_2)] + \frac{2}{9} s^{\Sigma^+}(x_1) \bar{s}(x_2) \}. \tag{28}$$

Furthermore, we introduce the ratio

$$T_V(x_1, x_2) = \frac{\tilde{\sigma}^+(x_1, x_2)}{\tilde{\sigma}^-(x_1, x_2)} = \frac{\frac{4}{9} \frac{u(x_1)}{s(x_1)} \Sigma^+ + \kappa(x_2)}{\frac{1}{9} \frac{u(x_1)}{s(x_1)} \Sigma^+ + \kappa(x_2)}, \tag{29}$$

where the ratio  $\kappa(x_2) = 2\bar{s}(x_2)/(\bar{u}(x_2) + \bar{d}(x_2))$ , which denotes the strange quark content of the nucleon.  $\kappa = 2\bar{s}/(\bar{u} + \bar{d})$  with  $x_2$  in the quark distributions being integrated has been determined experimentally in neutrino-induced charm production[27, 28, 29] to be in the range  $0.373^{+0.048}_{-0.041} \pm 0.018 \leq \kappa \leq 0.57 \pm 0.09$ . Actually, we find that the ratio  $\kappa(x_2)$  varies from 0.547 to 0.404 while  $x_2$  increasing from 0.001 to 0.7 according to the parameterizations of CTEQ [30]. We take  $x_2 = 0.3$  and then the value of  $\kappa(x_2)$  is 0.44, the predictions of  $T_V$  both in pQCD based and SU(6) diquark spectator models are shown in Fig. 9. The deviation between pQCD and diquark predictions for  $T_V$  is large enough in order to be used to test the flavor structure of  $\Sigma^\pm$ . We point out here that the above  $T_V(x_1, x_2)$  is only one example for the quantities that could show the difference between the two predictions, other quantities, such as  $\frac{\sigma(\Sigma^+ p)}{\sigma(\Sigma^+ n)}$ , could be an alternative quantity to test different predictions.

The use of the variables  $x_1$  and  $x_2$  is convenient for theoretical calculations and they signify the light-cone momentum fractions carried by the two colliding quarks in the beam hadron and target hadron. In the experimental measurements, it is convenient to use the experimental variables  $\tau = M^2/s$ , where  $M$  is the mass of the dilepton pair and  $s$  is the square of the total energy in the center of mass frame, and  $y$ , which is the rapidity of the dilepton pair, instead of the variables  $x_1$  and  $x_2$ . The two variables  $\tau$  and  $y$ , when expressed in terms of  $x_1$  and  $x_2$ , read

$$\begin{aligned}\tau &= x_1 x_2; \\ y &= \frac{1}{2} \ln\left(\frac{x_1}{x_2}\right),\end{aligned}\tag{30}$$

from which we get the two variables  $x_1$  and  $x_2$  in terms of  $\tau$  and  $y$

$$\begin{aligned}x_1 &= e^y \sqrt{\tau}; \\ x_2 &= e^{-y} \sqrt{\tau}.\end{aligned}\tag{31}$$

Thus we can express the quantity  $T_V$  as a function of  $\tau$  and  $y$ . It will be helpful if we can measure  $T_V(\tau, y)$  near the experimentally most accessible values of  $\tau$  and  $y$ , and also find significant differences between the predictions of the two models. We present  $T_V(\tau, y)$  in Figs. 10-11 for two cases: (i) at fixed  $y = 0$  by using  $\tau$  as a variable in Fig. 10, and (ii) at fixed  $\tau = 0.02$  by using  $y$  as a variable in Fig. 11. We find significant differences between the two predictions, thus it is possible to check the  $\Sigma^\pm$  flavor structure by measuring the quantity  $T_V(\tau, y)$ .

In principle we may extend the discussion to the case where the charged octet baryon  $\Xi^-$  is used as the beam. In this case  $s$  is the dominant valence quark and  $d$  is the less dominant valence quark at large  $x$  inside  $\Xi^-$ . Thus for the Drell-Yan process

$$\Xi^- N \rightarrow l^+ l^- X,\tag{32}$$

the cross sections can be written as,

$$\begin{aligned}\sigma(\Xi^- p) &= \frac{8\pi\alpha^2}{9\sqrt{\tau}} K(x_1, x_2) \left\{ \frac{4}{9} [u^{\Xi^-}(x_1)\bar{u}(x_2) + \bar{u}^{\Xi^-}(x_1)u(x_2)] \right. \\ &+ \frac{1}{9} [d^{\Xi^-}(x_1)\bar{d}(x_2) + \bar{d}^{\Xi^-}(x_1)d(x_2)] \\ &+ \left. \frac{1}{9} [s^{\Xi^-}(x_1)\bar{s}(x_2) + \bar{s}^{\Xi^-}(x_1)s(x_2)] \right\},\end{aligned}\tag{33}$$

and

$$\begin{aligned}
\sigma(\Xi^- n) &= \frac{8\pi\alpha^2}{9\sqrt{\tau}} K(x_1, x_2) \left\{ \frac{4}{9} [u^{\Xi^-}(x_1) \bar{d}(x_2) + \bar{u}^{\Xi^-}(x_1) d(x_2)] \right. \\
&+ \frac{1}{9} [d^{\Xi^-}(x_1) \bar{u}(x_2) + \bar{d}^{\Xi^-}(x_1) u(x_2)] \\
&+ \left. \frac{1}{9} [s^{\Xi^-}(x_1) \bar{s}(x_2) + \bar{s}^{\Xi^-}(x_1) s(x_2)] \right\}. \tag{34}
\end{aligned}$$

Considering the fact that the valence quarks  $s$  and  $d$  dominate in the  $\Xi^-$  at large  $x$ , we obtain

$$\tilde{\sigma}^p(x_1, x_2) = \frac{8\pi\alpha^2}{9\sqrt{\tau}} K(x_1, x_2) \left\{ \frac{1}{9} d^{\Xi^-}(x_1) \bar{d}(x_2) + \frac{1}{9} s^{\Xi^-}(x_1) \bar{s}(x_2) \right\}; \tag{35}$$

$$\tilde{\sigma}^n(x_1, x_2) = \frac{8\pi\alpha^2}{9\sqrt{\tau}} K(x_1, x_2) \left\{ \frac{1}{9} d^{\Xi^-}(x_1) \bar{u}(x_2) + \frac{1}{9} s^{\Xi^-}(x_1) \bar{s}(x_2) \right\}, \tag{36}$$

from which we have

$$\Delta\sigma = \tilde{\sigma}^p(x_1, x_2) - \tilde{\sigma}^n(x_1, x_2) = \frac{8\pi\alpha^2}{9\sqrt{\tau}} K(x_1, x_2) \left\{ \frac{1}{9} d^{\Xi^-}(x_1) [\bar{d}(x_2) - \bar{u}(x_2)] \right\}, \tag{37}$$

where the behavior of  $\bar{d}(x_2) - \bar{u}(x_2)$  is relatively well known from available studies on the Gottfried sum rule violation [4]. Thus the valence quark distribution  $d^{\Xi^-}(x)$  can be measured by using Eq. (37), and then substitute the measured  $d^{\Xi^-}(x)$  into Eq. (35) or (36) one can obtain the dominant valence quark  $s^{\Xi^-}(x)$  and check different predictions, if the data precision is high enough.

We would like to mention that in principle it should be possible to measure the spin structure of  $\Sigma^\pm$  from processes in which polarized  $\Sigma^\pm$  beams are involved, such as the spin-dependent Drell-Yan process. However, it is difficult to obtain polarized  $\Sigma^\pm$  beams. Therefore, it might be comparatively easier to use various  $\Sigma^\pm$  fragmentation processes as has been suggested for the  $\Lambda$  case [12, 13, 17] to study the spin and flavor structure of  $\Lambda^\pm$ , though this may suffer from uncertainties in the connections between the quark distributions and fragmentation functions. The spin structure of  $\Sigma^\pm$  can be measured from polarized  $\Sigma^\pm$  fragmentations in processes such as  $e^+e^-$  annihilation near the  $Z$ -pole and semi-inclusive deep inelastic scattering.

## 4 Summary

We found in this paper that  $\Lambda$  has the most significant difference in the flavor structure at large  $x$ , compared to that of other octet baryons, between the SU(6) quark spectator diquark model and the pQCD based model, and this supports the conclusion in a previous study [12] that the  $\Lambda$  can provide a new domain to test different models concerning the flavor and spin structure of the nucleon. However, for the  $\Lambda$  we still need a connection between the quark distributions inside the  $\Lambda$  and a quark fragmentation into a  $\Lambda$ , due to the fact that  $\Lambda$  is a charge neutral and therefore cannot be used as beam and its short lifetime makes it also difficult to serve as the target. In order to avoid the theoretical and experimental uncertainties concerning the connection between quark distributions and quark fragmentations, it is meaningful to find a charged baryon with also different flavor and spin structure between the two models. In order to test the flavor structure of octet baryons, we turn our attention in this paper on the flavor structure of  $\Sigma^\pm$ , which has the most significant difference between the two models at medium to large  $x$ . The ratio  $T_V$  of Drell-Yan total cross section of  $\Sigma^+$  beam to that of  $\Sigma^-$  beam to the isoscalar targets is sensitive to different models. The measurement of  $T_V$  can offer further information for a distinction between different predictions concerning the flavor structure of octet baryons. It is more interesting that the  $\Lambda$  and  $\Sigma^0$  have complete different flavor and spin structure though they are composed of same flavor quarks. The  $\Sigma^\pm$  have similar flavor structure compared to that of  $\Sigma^0$ , thus measurement of  $\Sigma^\pm$  is also helpful for our understanding of the  $\Sigma^0$  structure.

**Acknowledgments:** This work is partially supported by Fondecyt (Chile) postdoctoral fellowship 3990048, by Fondecyt (Chile) grant 1990806 and by a Cátedra Presidencial (Chile), and by National Natural Science Foundation of China under Grant Numbers 19605006, 19875024, 19775051, and 19975052.

## References

- [1] For reviews, see, e.g., H.-Y. Cheng, Int. J. Mod. Phys. **A** **11** (1996) 5109; G.P. Ramsey, Prog. Part. Nucl. Phys. **39** (1997) 599. For a recent discussion, see, B.-Q. Ma, I. Schmidt, and J. Soffer, Phys. Lett. **B** **441** (1998) 461.
- [2] S.J. Brodsky, J. Ellis, and M. Karliner, Phys. Lett. **B** **206** (1988) 309; J. Ellis and M. Karliner, Phys. Lett. **B** **213** (1988) 73; **B** **341** (1995) 397.
- [3] See, e.g., S.J. Brodsky and B.-Q. Ma, Phys. Lett. **B** **381** (1996) 317, and references therein.
- [4] For a recent review, see, e.g., S. Kumano, Phys. Rep. **303** (1998) 183.
- [5] B.-Q. Ma, Phys. Lett. **B** **274** (1992) 111; C. Boros, J.T. Londergan, and A.W. Thomas, Phys. Rev. Lett. **81** (1998) 4075.
- [6] G.R. Farrar and D.R. Jackson, Phys. Rev. Lett. **35** (1975) 1416.
- [7] R. Carlitz, Phys. Lett. **B** **58** (1975) 345; J. Kaur, Nucl. Phys. **B** **128** (1977) 219; A. Schäfer, Phys. Lett. **B** **208** (1988) 175.
- [8] S.J. Brodsky, M. Burkardt, and I. Schmidt, Nucl. Phys. **B** **441** (1995) 197.
- [9] B.-Q. Ma, Phys. Lett. **B** **375** (1996) 320.
- [10] W. Melnitchouk and A.W. Thomas, Phys. Lett. **B** **377** (1996) 11.
- [11] U.K. Yang and A. Bodek, Phys. Rev. Lett. **82** (1999) 2467.
- [12] B.-Q. Ma, I. Schmidt, and J.-J. Yang, Phys. Lett. **B** **477** (2000) 107.
- [13] B.-Q. Ma, I. Schmidt, and J.-J. Yang, Phys. Rev. **D** **61** (2000) 034017.
- [14] The HERMES Collab., A. Airapetian *et al.*, hep-ex/9911017.
- [15] V.N. Gribov and L.N. Lipatov, Phys. Lett. **B** **37** (1971) 78; Sov. J. Nucl. Phys. **15** (1972) 675.

- [16] S.J. Brodsky and B.-Q. Ma, Phys. Lett. **B 392** (1997) 452.
- [17] B.-Q. Ma and J. Soffer, Phys. Rev. Lett. **82** (1999) 2250.
- [18] B.-Q. Ma, J. Phys. **G 17** (1991) L53;  
B.-Q. Ma and Q.-R. Zhang, Z. Phys. **C 58** (1993) 479.
- [19] S. J. Brodsky, T. Huang, and G. P. Lepage, in *Particles and Fields-2*, Proceedings of the Banff Summer Institute, Banff, Alberta, 1981, edited by A. Z. Capri and A. N. Kamal (Plenum, New York, 1983), p. 143.
- [20] C. Boros and A. W. Thomas, Phys. Rev. **D 60** (1999) 074017.
- [21] SM Collab., D. Adams et al., Phys. Lett. **B 357** (1995) 248.
- [22] Particle Data Group, R. M. Barnett et al., Phys. Rev. **D 54** (1996) 1.  
See, e.g., C. Boros and Z. Liang, Phys. Rev. **D 57** (1998) 4491.
- [23] SM Collab., B. Adeva *et al.*, Phys. Lett. **B 369** (1996) 93; **B 420** (1998) 180.
- [24] The HERMES Collab., K. Ackerstaff et al., Phys. Lett. **B 484** (1999) 123.
- [25] For a recent review, see, e.g., P.L. McGaughey, J.M. Moss, and J.C. Peng, Ann. Rev. Nucl. Part. Sci. **49** (1999) 217.
- [26] M. Alberg *et al.*, Phys. Lett. **B 389** (1996) 367.
- [27] H. Abromowicz et al., Z. Phys. **C 15** (1982) 19.
- [28] C. Foudas et al. Phys. Rev. Lett. **64** (1990) 1207; M.H. Shaevitz, Nucl. Phys. B (Proc. Suppl.) **19** (1991) 270; S.A. Rabinowitz et al., Phys. Rev. Lett. **70** (1993) 134; A.O. Bazarko et al., Z. Phys. **C 65** (1995) 189.
- [29] B. Strongin et al., Phys. Rev. **D 43** (1991) 2778.
- [30] H.L. Lai et al., Phys. Rev. **D 51** (1995) 4763; Phys. Rev. **D 55** (1997) 1280.

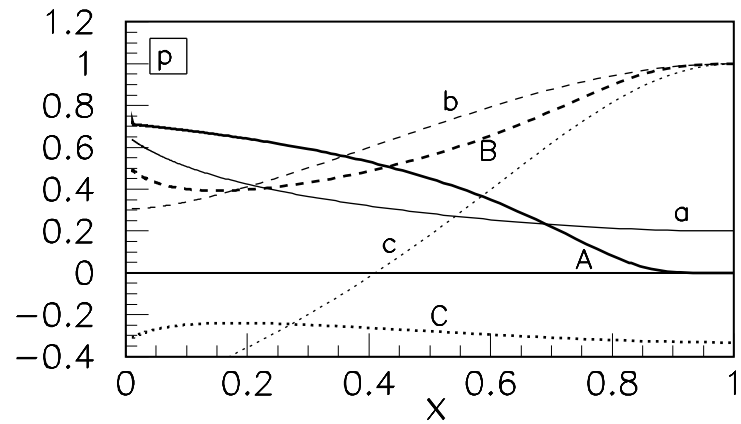


Figure 1:  $A = (\frac{q_2}{q_1})^{Diquark}$ ,  $B = (\frac{\Delta q_1}{q_1})^{Diquark}$ ,  $C = (\frac{\Delta q_2}{q_2})^{Diquark}$ ,  $a = (\frac{q_2}{q_1})^{pQCD}$ ,  $b = (\frac{\Delta q_1}{q_1})^{pQCD}$  and  $c = (\frac{\Delta q_2}{q_2})^{pQCD}$  for the proton in which  $q_1 = u$  and  $q_2 = d$ .

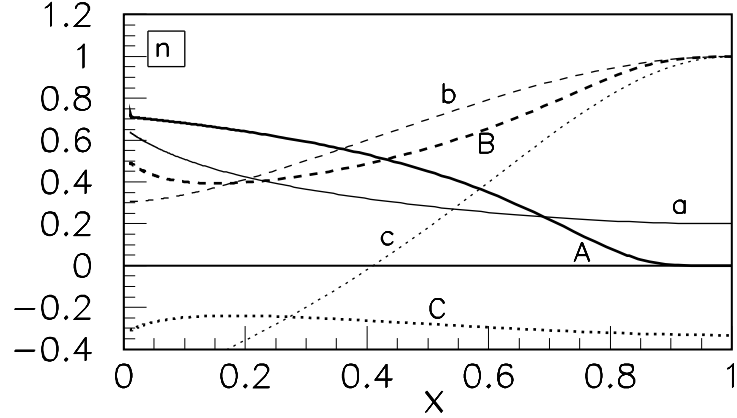


Figure 2:  $A = (\frac{q_2}{q_1})^{\text{Diquark}}$ ,  $B = (\frac{\Delta q_1}{q_1})^{\text{Diquark}}$ ,  $C = (\frac{\Delta q_2}{q_2})^{\text{Diquark}}$ ,  $a = (\frac{q_2}{q_1})^{\text{pQCD}}$ ,  $b = (\frac{\Delta q_1}{q_1})^{\text{pQCD}}$  and  $c = (\frac{\Delta q_2}{q_2})^{\text{pQCD}}$  for the neutron in which  $q_1 = d$  and  $q_2 = u$ .

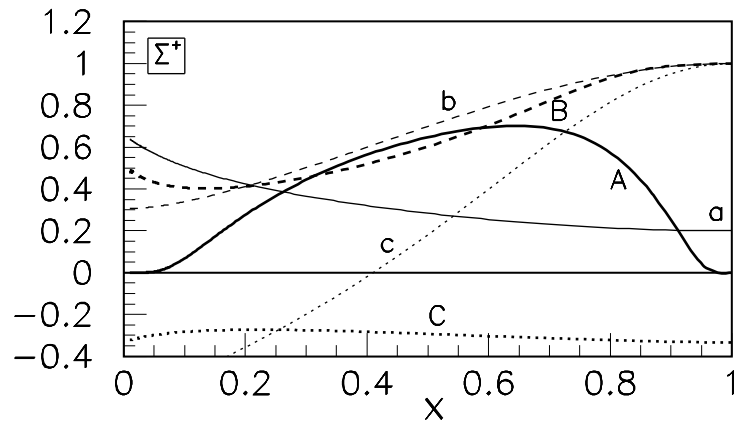


Figure 3:  $A = (\frac{q_2}{q_1})^{\text{Diquark}}$ ,  $B = (\frac{\Delta q_1}{q_1})^{\text{Diquark}}$ ,  $C = (\frac{\Delta q_2}{q_2})^{\text{Diquark}}$ ,  $a = (\frac{q_2}{q_1})^{\text{pQCD}}$ ,  $b = (\frac{\Delta q_1}{q_1})^{\text{pQCD}}$  and  $c = (\frac{\Delta q_2}{q_2})^{\text{pQCD}}$  for the  $\Sigma^+$  in which  $q_1 = u$  and  $q_2 = s$ .

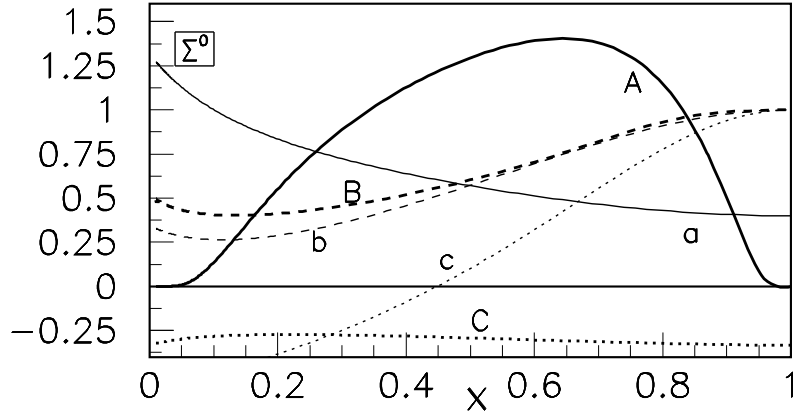


Figure 4:  $A = (\frac{q_2}{q_1})^{\text{Diquark}}$ ,  $B = (\frac{\Delta q_1}{q_1})^{\text{Diquark}}$ ,  $C = (\frac{\Delta q_2}{q_2})^{\text{Diquark}}$ ,  $a = (\frac{q_2}{q_1})^{\text{pQCD}}$ ,  $b = (\frac{\Delta q_1}{q_1})^{\text{pQCD}}$  and  $c = (\frac{\Delta q_2}{q_2})^{\text{pQCD}}$  for the  $\Sigma^0$  in which  $q_1 = u(d)$  and  $q_2 = s$ .

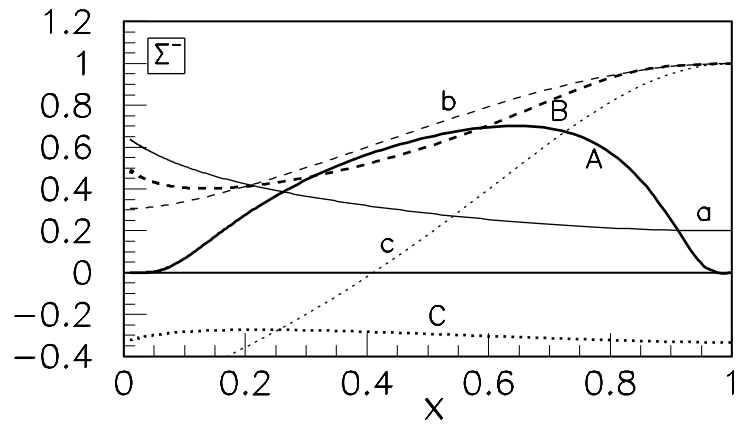


Figure 5:  $A = (\frac{q_2}{q_1})^{\text{Diquark}}$ ,  $B = (\frac{\Delta q_1}{q_1})^{\text{Diquark}}$ ,  $C = (\frac{\Delta q_2}{q_2})^{\text{Diquark}}$ ,  $a = (\frac{q_2}{q_1})^{\text{pQCD}}$ ,  $b = (\frac{\Delta q_1}{q_1})^{\text{pQCD}}$  and  $c = (\frac{\Delta q_2}{q_2})^{\text{pQCD}}$  for the  $\Sigma^-$  in which  $q_1 = d$  and  $q_2 = s$ .

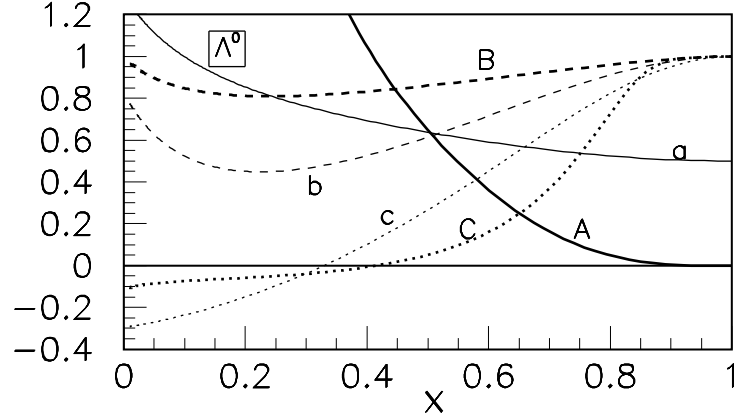


Figure 6:  $A = (\frac{q_2}{q_1})^{Diquark}$ ,  $B = (\frac{\Delta q_1}{q_1})^{Diquark}$ ,  $C = (\frac{\Delta q_2}{q_2})^{Diquark}$ ,  $a = (\frac{q_2}{q_1})^{pQCD}$ ,  $b = (\frac{\Delta q_1}{q_1})^{pQCD}$  and  $c = (\frac{\Delta q_2}{q_2})^{pQCD}$  for the  $\Lambda^0$  in which  $q_1 = s$  and  $q_2 = u(d)$ .

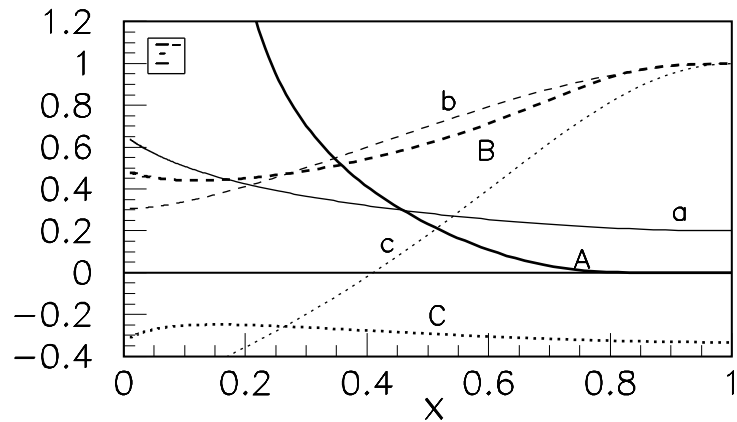


Figure 7:  $A = (\frac{q_2}{q_1})^{Diquark}$ ,  $B = (\frac{\Delta q_1}{q_1})^{Diquark}$ ,  $C = (\frac{\Delta q_2}{q_2})^{Diquark}$ ,  $a = (\frac{q_2}{q_1})^{pQCD}$ ,  $b = (\frac{\Delta q_1}{q_1})^{pQCD}$  and  $c = (\frac{\Delta q_2}{q_2})^{pQCD}$  for the  $\Xi^-$  in which  $q_1 = s$  and  $q_2 = d$ .

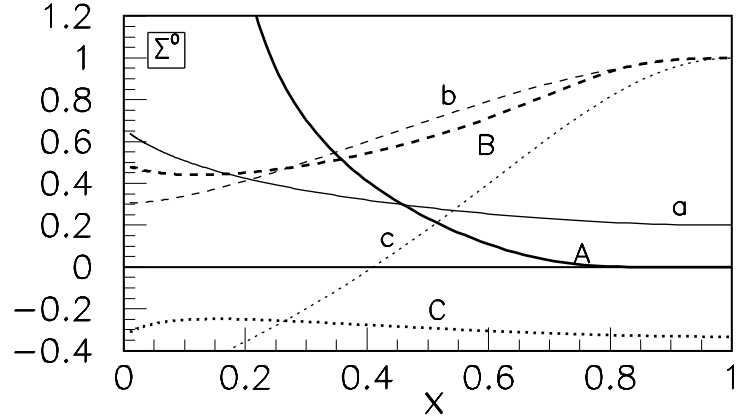


Figure 8:  $A = (\frac{q_2}{q_1})^{Diquark}$ ,  $B = (\frac{\Delta q_1}{q_1})^{Diquark}$ ,  $C = (\frac{\Delta q_2}{q_2})^{Diquark}$ ,  $a = (\frac{q_2}{q_1})^{pQCD}$ ,  $b = (\frac{\Delta q_1}{q_1})^{pQCD}$  and  $c = (\frac{\Delta q_2}{q_2})^{pQCD}$  for the  $\Xi^0$  in which  $q_1 = s$  and  $q_2 = u$ .

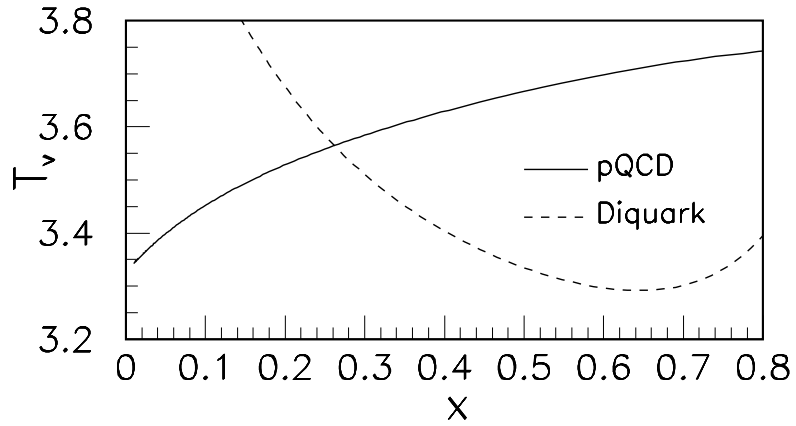


Figure 9: The  $T_V(x_1, x_2)$  in the SU(6) quark-diquark and pQCD based Models at fixed  $x_2 = 0.3$  as a function of  $x = x_1$ .

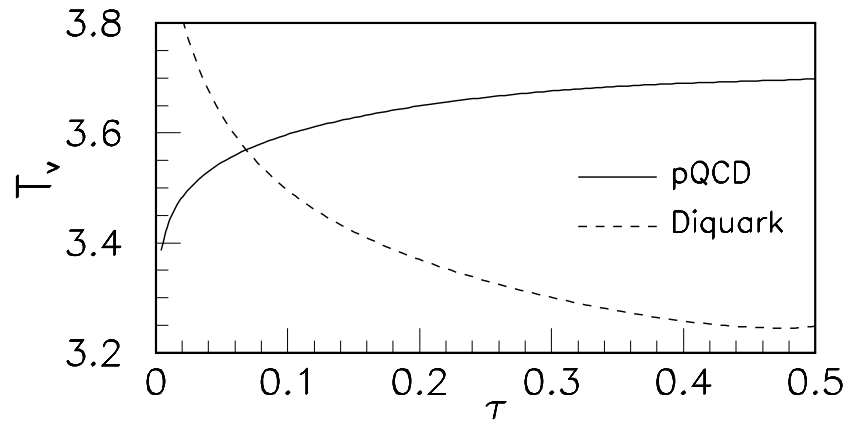


Figure 10: The  $T_V(\tau, y)$  in the SU(6) quark-diquark and pQCD based Models at fixed  $y = 0$  as a function of  $\tau$ .

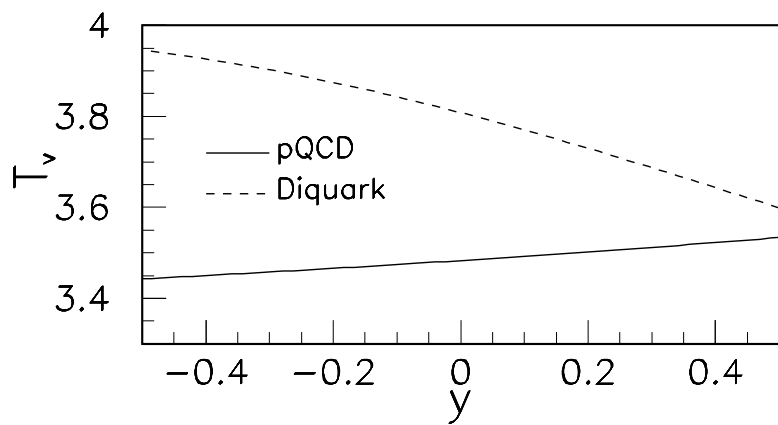


Figure 11: The  $T_V(\tau, y)$  in the SU(6) quark-diquark and pQCD based Models at fixed  $\tau = 0.02$  as a function of  $y$ .